REPORT DOCUMENTATION PAGE

AFRL-SR-AR-TR-03-

0340

1. AGENCY USE ONLY (*Leave Blank*)	2. REPORT DATE July 3, 2003	3. REPORT TYPE AND DATES COVERED Final Report: 0815/02 thru July 3, 2003

4. TITLE AND SUBTITLE
indium Gallium Arsenide Nitride Quantum Dots for High Speed Infrared Emitters

5. FUNDING NUMBERS
F49620-02-C-0068

6. AUTHORS
Dr. Aaron Moy

7. PERFORMING ORGANIZATION NAME(S) AND ADDRESS(ES)
SVT Associates, Inc.
7620 Executive Drive
Eden Prairie, MN 55344

8. PERFORMING ORGANIZATION REPORT NUMBER
Final

9. SPONSORING / MONITORING AGENCY NAME(S) AND ADDRESS(ES)
Air Force Office of Scientific Research
4015 Wilson Blvd., Room 713
Arlington, VA 22203

10. SPONSORING / MONITORING AGENCY REPORT NUMBER

11. SUPPLEMENTARY NOTES

12a. DISTRIBUTION / AVAILABILITY STATEMENT
Approved for Public Release; Distribution Unlimited

12b. DISTRIBUTION CODE

13. ABSTRACT *(Maximum 200 words)*

Report developed under SBIR contract for Topic BMDO02-011 to investigate InGaAsN quantum dots for application to high speed infrared emitters. The Phase I study successfully fabricated and characterized both InGaAs and InGaAsN quantum dots. Atomic force microscopy and transmission electron microscopy verfied the structural properties of the dots. Infrared photonic emission from these dots was acheived with samples at both 77 K and room temperature. The feasibility of using InGaAsN quantum dots for infrared emitters has been demonstrated and continued Phase II effort is warranted.

14. SUBJECT TERMS SBIR Report			15. NUMBER OF PAGES 25
			16. PRICE CODE
17. SECURITY CLASSIFICATION OF REPORT Unclassified	18. SECURITY CLASSIFICATION OF THIS PAGE Unclassified	19. SECURITY CLASSIFICATION OF ABSTRACT Unclassified	20. LIMITATION OF ABSTRACT UL

NSN 7540-01-280-5500

Standard Form 298 (Rev. 2-89)
Prescribed by ANSI Std. Z39-1
298-102

Executive Summary

This Phase I effort sought to investigate the creation of InGaAsN quantum dots (QDs) on GaAs substrates. Various GaAs substrates of different orientations were used including (100) on-axis, (100) cut 6° off-axis and (311). Growth conditions for QD formation were studied such as alloy composition and temperature. The presence of InGaAsN QDs were verified structurally using atomic force microscopy (AFM). Optical characterization of the dots was performed with photoluminescence (PL), where InGaAsN QDs were found to have room temperature photoemission at a wavelength > 1.66 micron. High resolution transmission electron microscopy (TEM) was also used to examine the QD formation.

Background

Quantum dots in semiconductors are areas of low bandgap energy material with a size in all three dimensions on the order of 100 Å or less, surrounded by a high bandgap energy barrier layer. When successfully fabricated, charge carriers (holes and electrons) can become trapped inside QDs and exhibit unique properties. For this program, we intend to apply $In_xGa_{1-x}As_yN_{1-y}$ as the quantum dot material.

$In_xGa_{1-x}As_yN_{1-y}$ is a novel quaternary III-V alloy. Its particular advantage is the fact that this material can have a low bandgap energy (~ 0.5 to 1.2 eV) while maintaining a crystal size and structure very similar to GaAs (Fig.1). The alloy requires only small amounts of nitrogen (< 4%) to achieve the desired properties. GaAs has a bandgap energy of 1.42 eV and GaAs processing technology is mature, so these materials can be combined to make $In_xGa_{1-x}As_yN_{1-y}$/GaAs quantum dots and barriers.

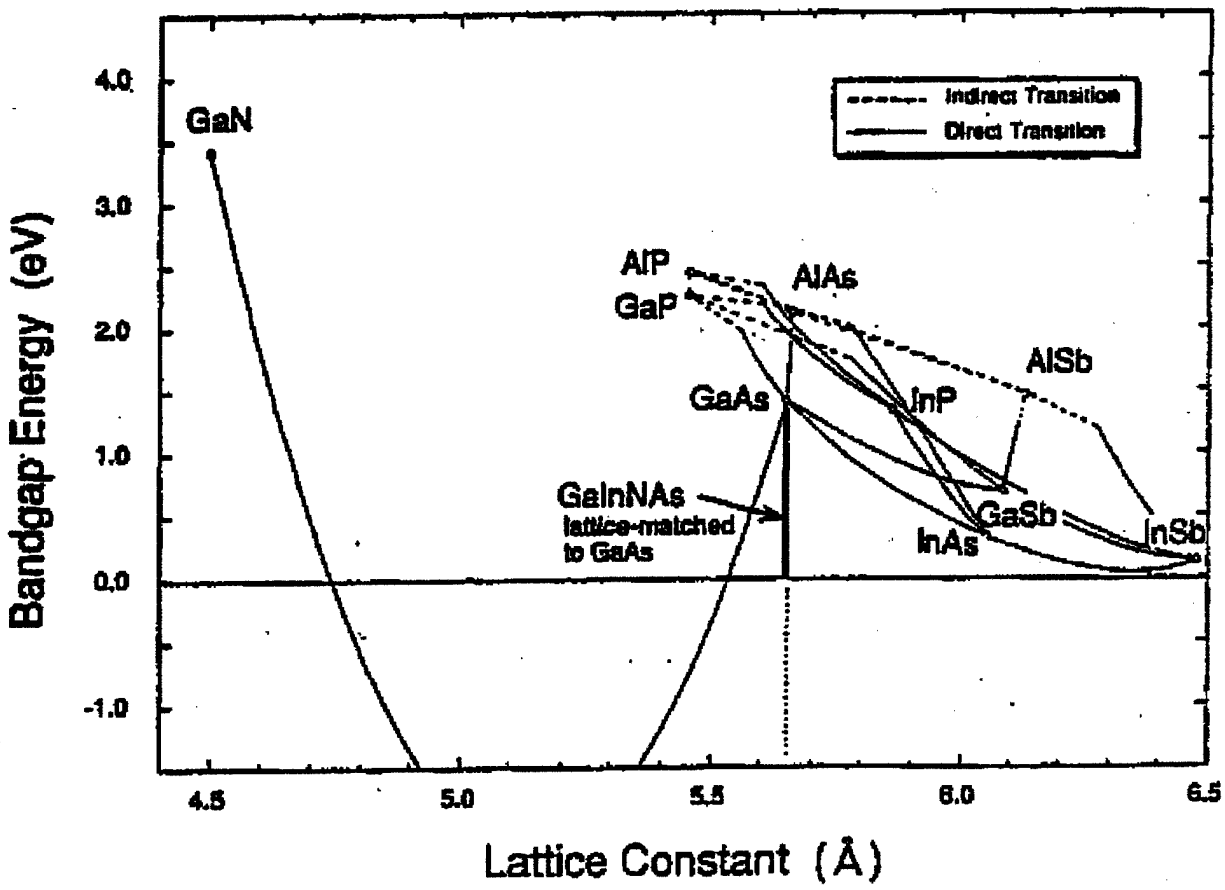

Figure 1. Diagram of lattice constant and bandgap energy in III-V alloy semiconductors. Of particular interest is the extreme bowing which occurs in the $GaAs_xN_{1-x}$ alloy for varying levels of N.

InAs(N) QDs on On-Axis GaAs

Initial experiments sought to compare InAs only dots with InAsN dots. Following the growth of 5000 Å of GaAs buffer layer, 1.5 monolayers of InAs were deposited at a substrate temperature of 480 °C. Some dot formation is seen in the atomic force micrograph of the surface (Fig. 2a). For comparison, 1.5 monolayers of InAsN were also deposited onto a different GaAs sample at the same conditions, except nitrogen was introduced using an N_2 RF plasma source. With the nitrogen added, the islands in the InAsN sample appear much larger and less dense than for InAs-only (Fig. 2b).

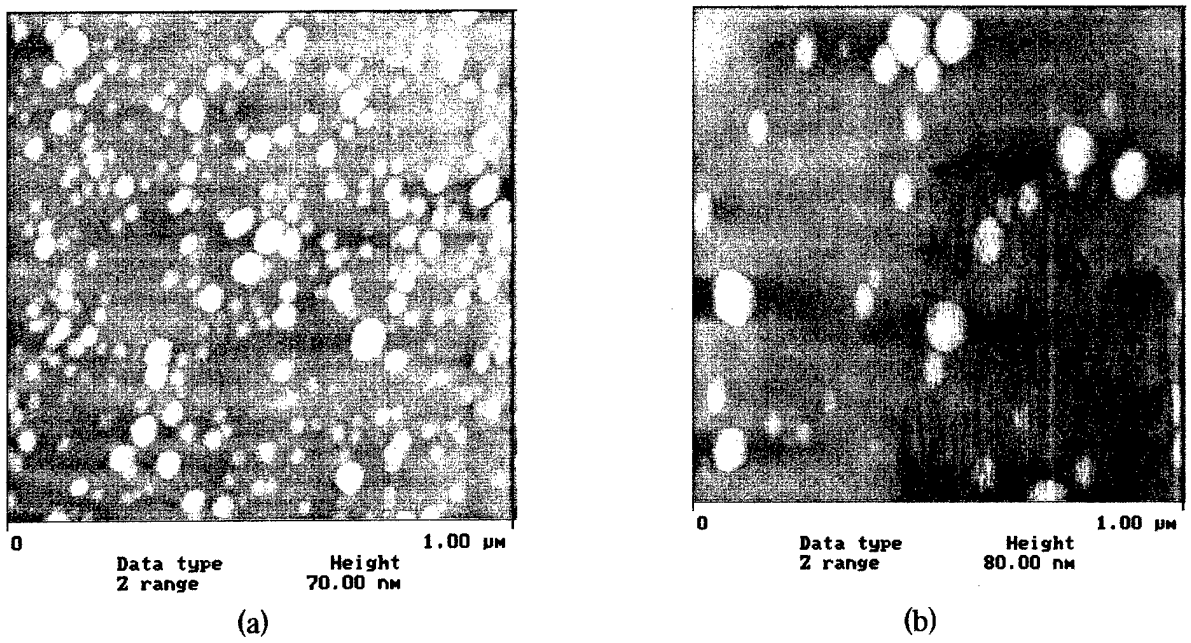

Figure 2. AFM images of a) InAs and b) InAsN 1.5 monolayers thick on GaAs.

In succeeding experiments, the thickness of the InAs(N) layer was increased to 3 monolayers, and the substrate temperature was increased to 500 °C. For the InAs-only layer, the density of QDs is greatly increased to ~ 2.8 x 10^{10} dots/cm^2 (Fig. 3). The AFM image shows two general size groups for the dots. Three monolayers of InAsN were deposited on a second sample using the RF plasma injector at 300 W and a system pressure of 6 x 10^{-7} torr. The InAsN dots are slightly smaller and more dense, ~ 3.3 x 10^{10} dots/cm^2, compared to InAs-only (Fig. 4a). As a control, 3 monolayers InAs was also deposited with inert nitrogen at a growth system pressure of 6 x 10^{-7} torr. The RF power was zero, so the N_2 molecules are expected to be inert and therefore not incorporate into the growth. The QDs created under inert N_2 conditions have a size distribution similar to the InAs-only control sample (Fig. 4b). From this series we can conclude that active N species does have an effect on InAsN QD growth.

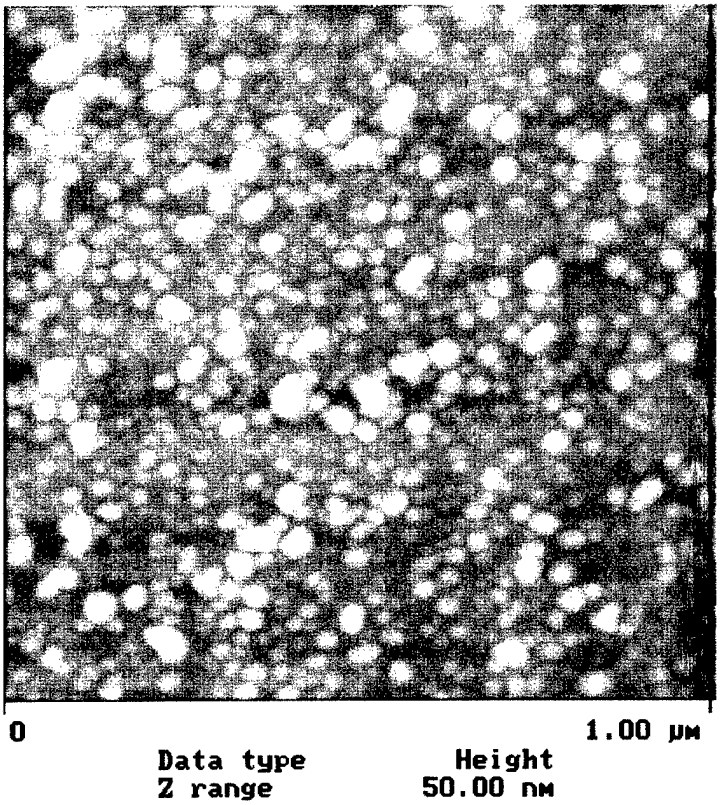

Figure 3. Quantum dots from 3 monolayers of InAs on GaAs at 500 °C.

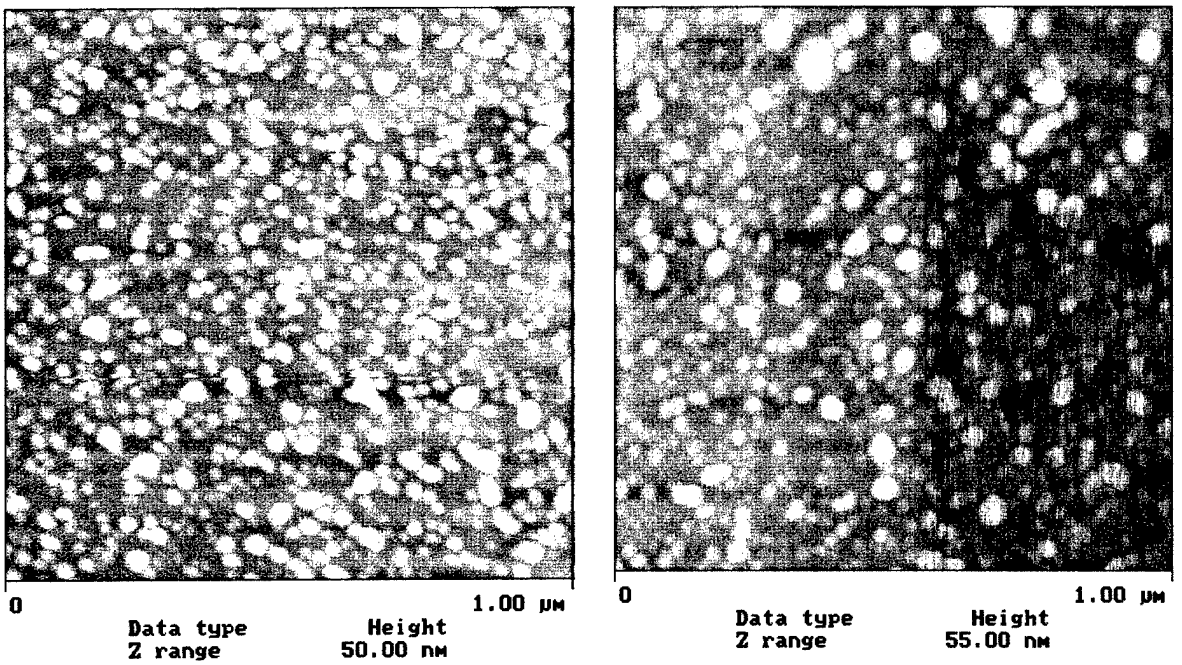

(a) (b)

Figure 4. Three monolayers of InAs(N) a) with RF nitrogen plasma on at 300 W and b) inert nitrogen gas, both at a growth system pressure of 6 x 10^{-7} torr.

InGaAs(N) QDs on On-Axis GaAs

InGaAs(N) QDs were then explored. Figure 5 displays 4 monolayers of $In_{0.58}Ga_{0.42}As$ on GaAs at 500 °C. The QD density has increased to 7.2 x 10^{10} dots/cm^2. Four monolayers of $In_{0.58}Ga_{0.42}AsN$ were then deposited on another sample with the RF plasma at 250 W and system pressure of 4 x 10^{-7} torr. The dot density increased slightly to 9.3 x 10^{10} dots/cm^2 (Fig. 6a). InGaAsN QDs of the same composition were grown at the same conditions except the substrate temperature was raised to 540 °C (Fig. 6b). The QD density decreased slightly to 7.8 x 10^{10} dots/cm^2 when compared with the 500 °C InGaAsN sample, and several large island regions developed.

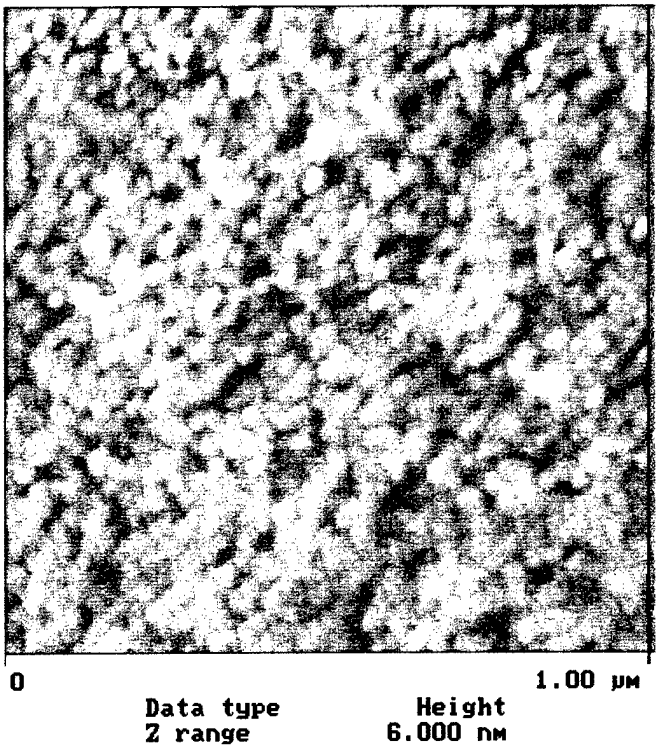

Figure 5. Quantum dots formed with 4 monolayers $In_{0.58}Ga_{0.42}As$ on GaAs at 500 °C.

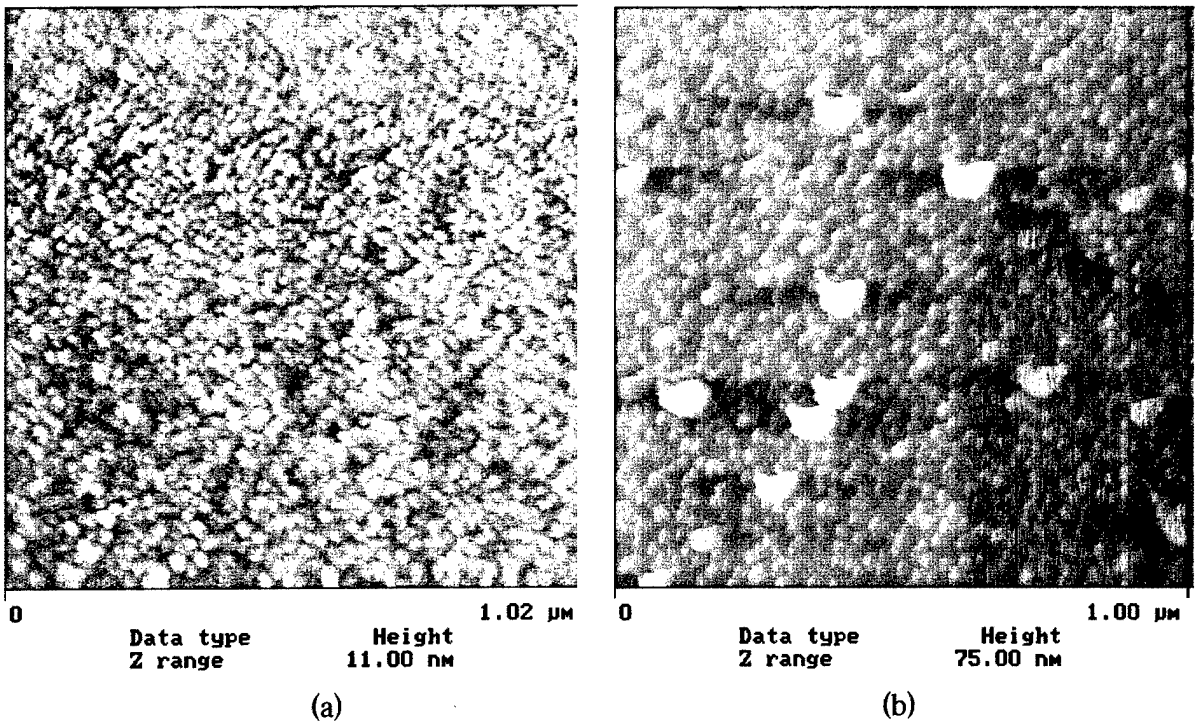

Figure 6. Quantum dots formed with 4 monolayers $In_{0.58}Ga_{0.42}AsN$ on GaAs at a) 500 °C and b) 540 °C using a nitrogen RF plasma at 250 W.

InGaAs(N) QDs on Off-Axis GaAs

The quantum dots reported thus far were grown on (100) on-axis GaAs wafers. This type of substrate offers a very flat, uniform surface. Substrates can be cut and polished differently, however, in "off-axis" orientations. When cut in this manner, the surface is not flat, but rather has terraces (Fig. 7). The step edges of these terraces create preferential bonding sites, which may help to influence the location and size of QD formation (Fig. 8). In addition to these wafers which were intentionally cut off-axis, other substrates were used which had a different crystal orientation, such as (311)-oriented. Due to the numbers and angles of dangling bonds at the surface, (x11)-oriented wafers have effective terrace structures which may also influence the QD growth (Fig. 9).

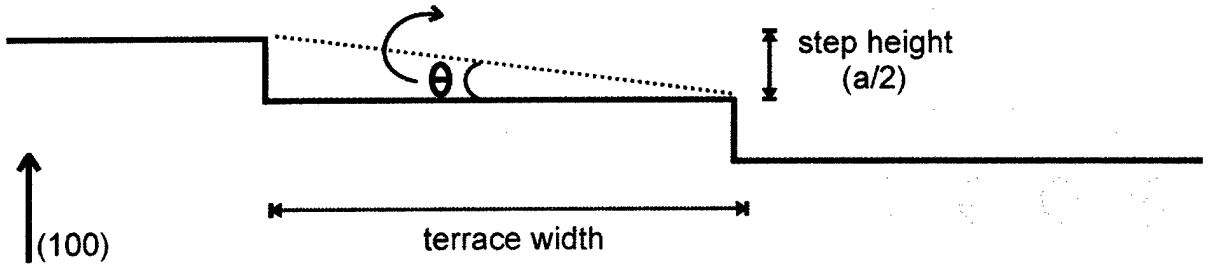

Figure 7. Side view of a (100)-oriented substrate intentionally cut slightly off-axis. The shallow cut results in a surface with terraced steps. Average height for each step is one atomic layer, which is one half the lattice constant. Terrace width is dependent on the cut angle.

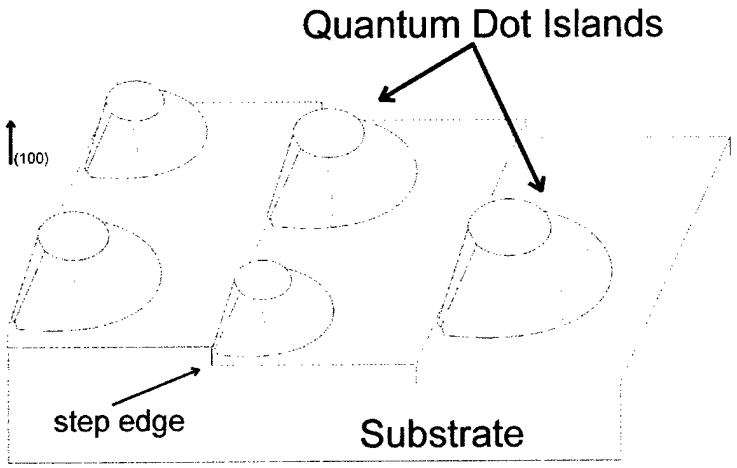

Figure 8.

Theorized rendition of quantum dot formation where the step edges on the surface of misoriented substrates influence the distribution, resulting in improved uniformity.

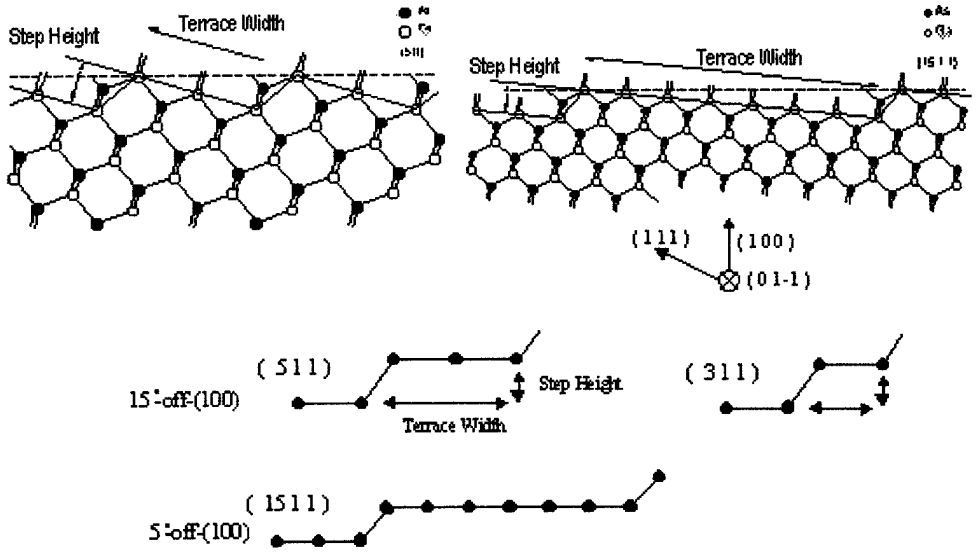

Figure 9. Differently tilted substrates viewed along the [011] direction showing different terrace widths. The heavy line highlights the (100) terrace structure.

Quantum dots growths were conducted on (100) GaAs substrates cut 6° toward the (110) direction. As a control sample, a 6 monolayer thick wetting layer of $In_{0.5}Ga_{0.5}As$ was deposited at 500 °C after growing a 0.5 micron GaAs buffer layer. The AFM image shows a very high areal density of QDs, approximately 1.1×10^{11} dots/cm^2 (Fig. 10). $In_{0.5}Ga_{0.5}AsN$ dots were then grown on separate samples at 500 °C substrate temperature and with the nitrogen RF plasma generator at 275 W. $In_{0.5}Ga_{0.5}AsN$ wetting layers of 6 and 8 monolayers were studied. AFM for the 6 monolayer InGaAsN sample reveal quantum dot formation (Fig. 11), though the areal density of 8.4×10^{10} dots/cm^2 is slightly less than the comparable InGaAs-only QD sample. Most of the QDs fall into the same size group in this sample. Comparing the InGaAs and InGaAsN QDs grown under the same nominal conditions, it is seen that the addition of nitrogen does have an effect. With nitrogen, the dot sizes are slightly larger, and the areal density is slightly smaller. Also, looking at the QD arrangement, the InGaAs-only dots have a strong coherence in terms of following common alignment directions as marked by the blue arrow in the AFM image (Fig. 10). Some alignment is also seen in the InGaAsN dots, though it is not as great.

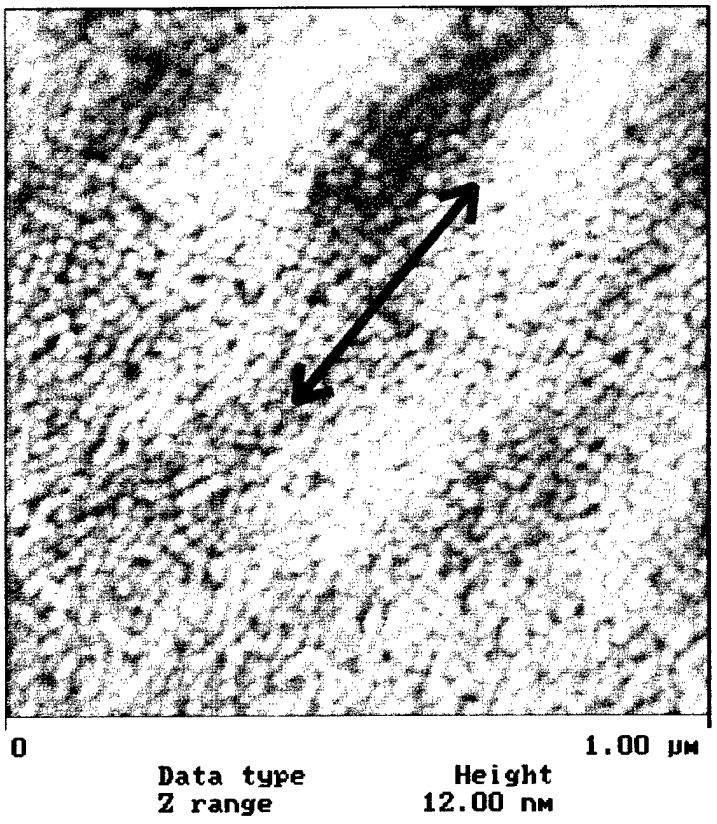

Figure 10.

$In_{0.5}Ga_{0.5}As$ quantum dots grown on (100) GaAs substrates cut 6° toward the (110). The wetting layer thickess was 6 monolayers. Common directional alignment is highlighted by the blue arrow.

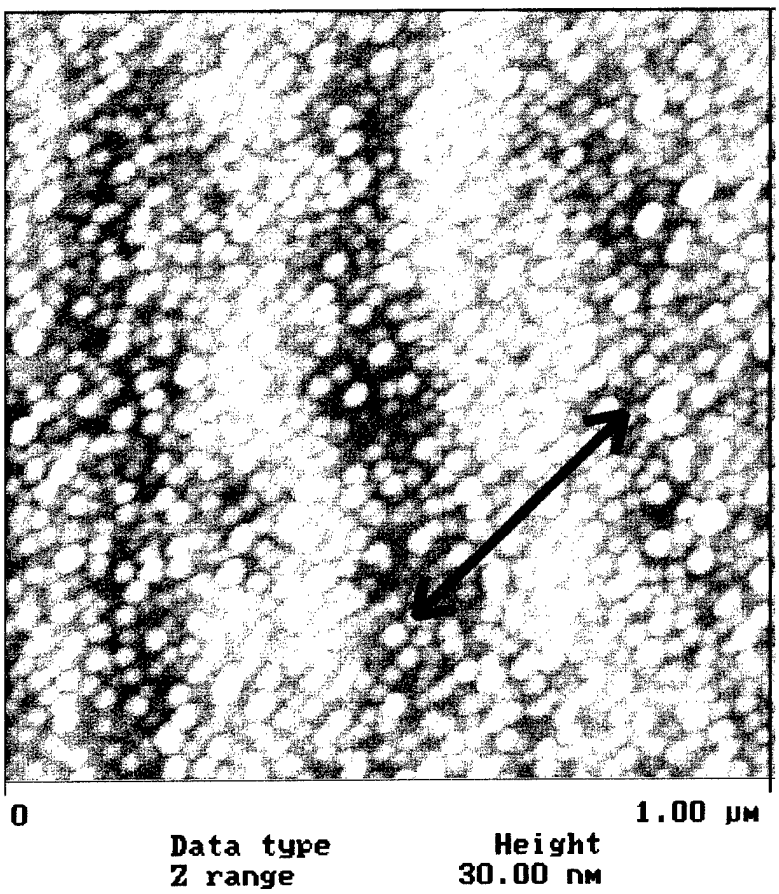

Figure 11.

$In_{0.5}Ga_{0.5}AsN$ quantum dots grown on (100) GaAs substrates cut 6° toward the (110). The wetting layer thickess was 6 monolayers. Some alignment is seen in the dot formation.

Also part of this series was an $In_{0.5}Ga_{0.5}AsN$ QD sample grown on the same type of off-axis substrate, but with 8 monolayers wetting layer thickness instead ot 6. Dots were again seen in the AFM image (Fig. 12), though the dot sizes fell into two general groups, large and small. There were approximately 1.7×10^{10} large dots/cm^2 and 4.8×10^{10} small dots/cm^2. Again, some preferential alignment direction is observed, particularly with the smaller dots. All three of these samples demonstrated some alignment of the QDs, likely due to the terraces on the off-axis substrate. The addition of N into the InGaAs wetting layer also appears to reduce the dot density. This would be consistent with the fact that adding nitrogen decreases the lattice constant of the InGaAsN alloy, which reduces the strain force, and strain force itself is what drives the QD formation.

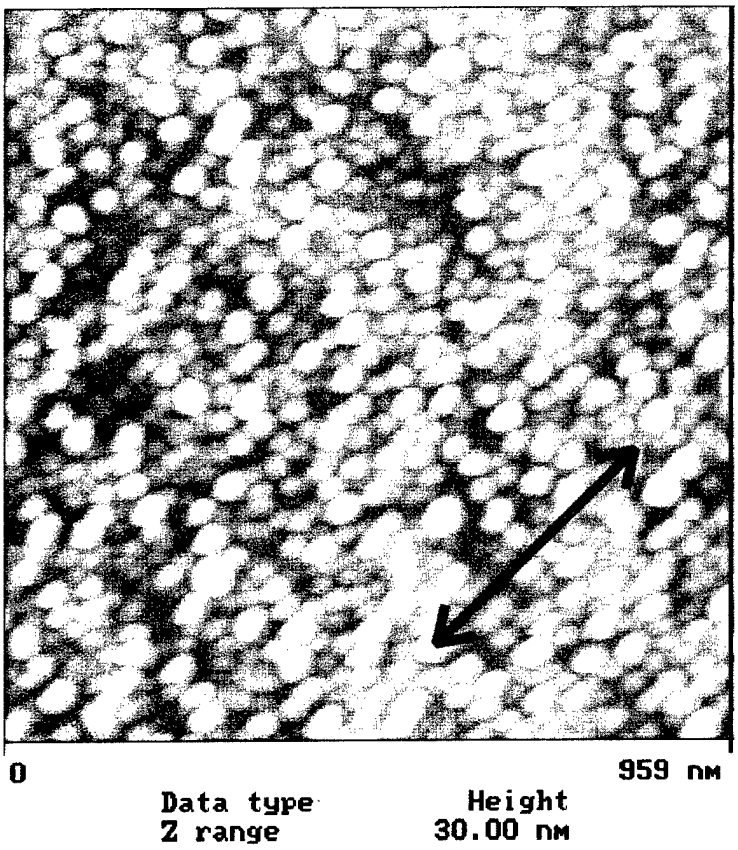

Figure 12.

$In_{0.5}Ga_{0.5}AsN$ quantum dots grown on (100) GaAs substrates cut 6° toward the (110). The wetting layer thickess was 8 monolayers. Again some alignment is seen in the dot formation.

InGaAs QD Deposition Scheme Study

In another series of growths, the In composition of the wetting layer was increased to $In_{0.57}Ga_{0.43}As$. Again, (100) GaAs substrates cut 6° toward the (110) were used. Only InGaAs dots were grown, but they were grown using different schemes. The higher relative indium level should increase the strain in the wetting layer, and thus affect the QD formation. Figure 13 displays the AFM image of the dots with 6 monolayers of growth. In this scheme, the In, Ga and As were applied simultaneously, as is normal in typical MBE technique. Dots are seen to form 2 size groups, though the areal density is not as high as in the previous samples. Some alignment is still present.

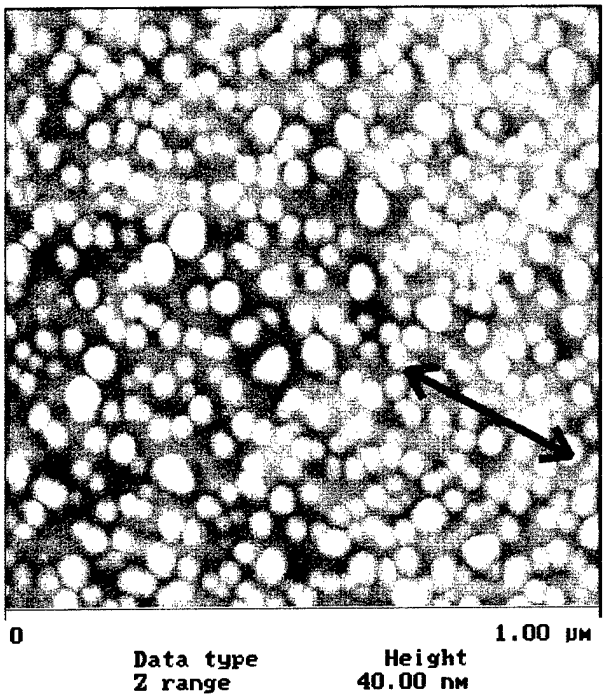

Figure 13.

$In_{0.57}Ga_{0.43}As$ quantum dots grown on (100) GaAs substrates cut 6° toward the (110). The wetting layer thickess was 6 monolayers.

For the next sample, the growth scheme used was modified. Following the GaAs buffer layer, 6 monolayers of In and Ga were deposited, but the As flux was not applied. Following the In and Ga deposition, 60 seconds of As-only flux was used. In this recipe, the group III (In, Ga) and group V (As) materials were deposited at separate times. From the AFM image it appears that large islands have formed, on top of which are quantum dots (Fig. 14). No obvious improvement in the dots is apparent.

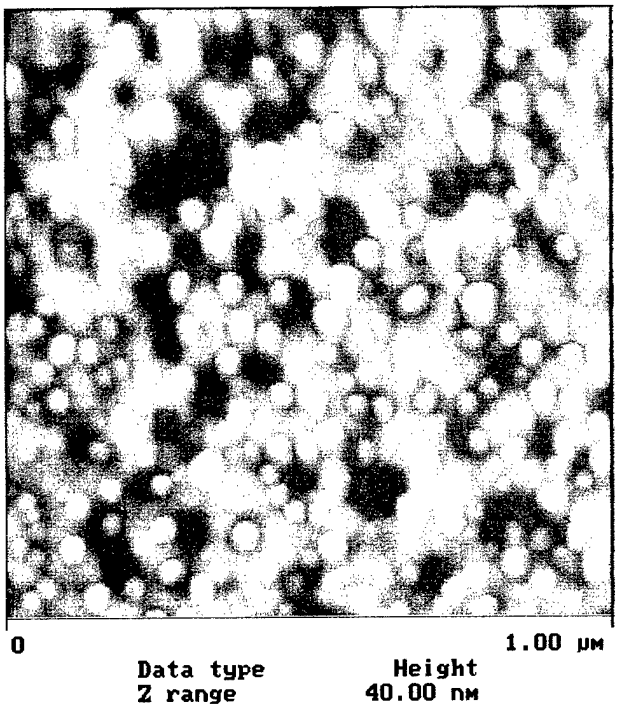

Figure 14.

$In_{0.57}Ga_{0.43}As$ quantum dots grown on (100) GaAs substrates cut 6° toward the (110). The In/Ga and As materials were deposited at separate times.

In another recipe, In/Ga and As were again deposited separately. However, the sequence used was 3 monolayers In/Ga, As for 30 seconds, 3 monolayers of In/Ga and lastly 30 seconds of As. This is similar to the method of the previous sample, except that the 6 total monolayers of In/Ga were split into two groups of 3 monolayers. The dots are smaller and more dense (Fig. 15), and there are several chains of dots which are aligned. Alignment here may be due to a combination of both the terrace steps and influence from a neighboring dot because not all the lines follow the same parallel direction.

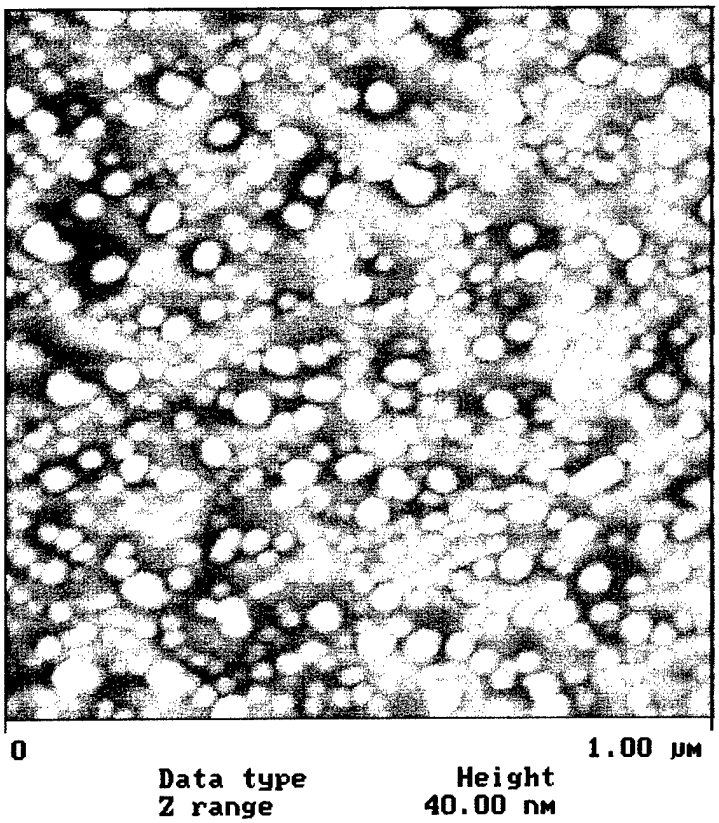

Figure 15.

$In_{0.57}Ga_{0.43}As$ quantum dot on off-axis GaAs. In/Ga deposition occurred in two separate groups of 3 monolayer thick layers, followed by 30 seconds each of As.

Last in this series was a sample with 6 monolayers of In/Ga deposited, followed by 60 seconds of As. In between the In/Ga and As sequences, however, a pause time of 10 seconds was inserted. During this period no MBE sources were exposed to the growth surface. This extra time allows for the In and Ga atoms to move laterally across the surface before As is applied. AFM of this sample reveals interesting formations (Fig. 16). There are many islands which consist of a large end and a small end. Moreover, the direction between the large and small ends are all in a

common direction. The sample should have been rotating during grown, so gravitational effects should have been homogenous. However, further experiments would be required to explain the nature of this island arrangement here. All the samples in this series consisted of nominally 6 monolayers of $In_{0.57}Ga_{0.43}As$. Based on the method used to deposit the wetting layers though, it is seen how different the resulting dots can be. This knowledge can be applied in future experiments.

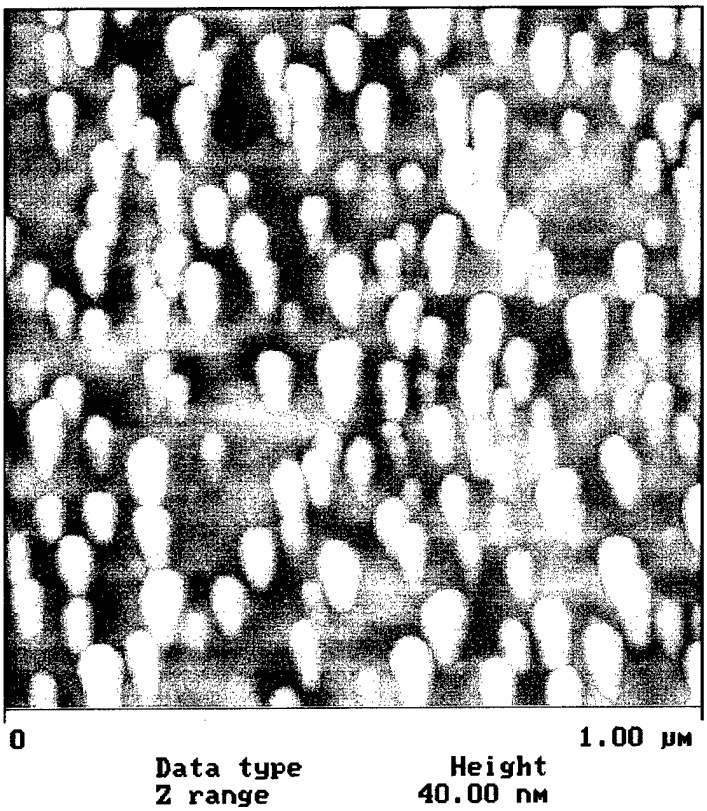

Figure 16.

$In_{0.57}Ga_{0.43}As$ quantum dot on off-axis GaAs. 6 monolayers of In/Ga deposition occurred, followed by 10 seconds of nothing and 60 seconds of As.

InGaAs Quantum Dots on (311) Substrate

Growths were conducted using a wetting layer of $In_{0.53}Ga_{0.47}As(N)$ on (311)-oriented GaAs. 6 monolayers of InGaAs-only were deposited on this type of substrate at 450 °C. As seen in the AFM image of Figure 17, only a few large islands formed. These islands do appear to have a pentagonal shape, influenced by the unique bonds present at the (311) surface. The sample growth conditions were repeated, but with the addition of nitrogen. Island sizes for the InGaAsN

wetting layer are smaller than InGaAs alone, but the size and density are not quite applicable to quantum dots.

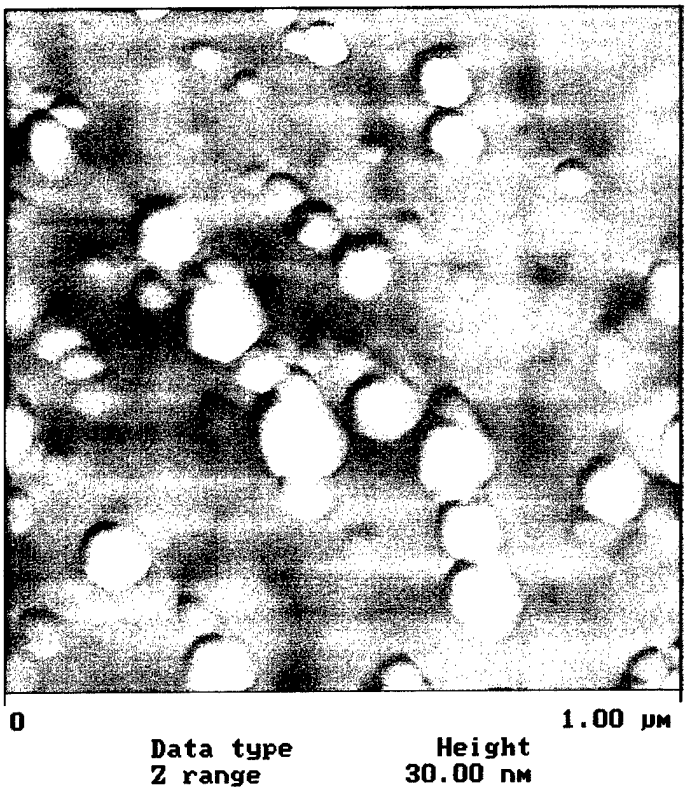

Figure 17

Islands from a 6 monolayer thick $In_{0.53}Ga_{0.47}As$ wetting layer grown on (311) GaAs substrate at 450 °C.

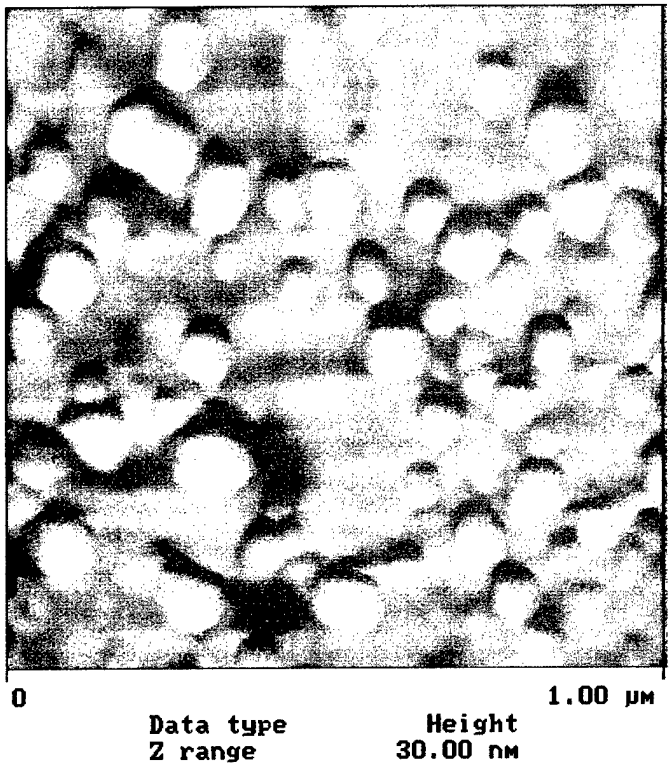

Figure 18

Islands from a 6 monolayer thick $In_{0.53}Ga_{0.47}AsN$ wetting layer grown on (311) GaAs substrate. The addition of nitrogen reduced the dot size.

Growth temperature was increased to 480 °C, and again 6 monolayers of $In_{0.53}Ga_{0.47}As(N)$ were deposited on (311)-oriented GaAs. Under these growth conditions, the QD size and density have been improved (Fig. 19). Compared to dots on (100) substrates, these dots are not quite round, but have polygonal forms due to the influence of the (311) surface. Additional effort can be applied in the Phase II to further reduce the dot size and increase areal density.

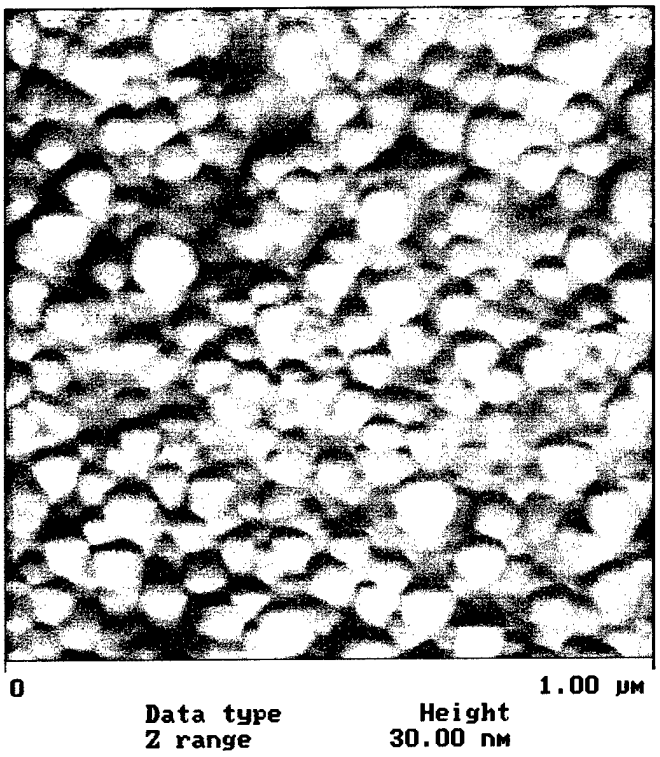

Figure 19

QDs from a 6 monolayer thick $In_{0.53}Ga_{0.47}AsN$ wetting layer grown on (311) GaAs substrate at 480 °C.

Multiple Layer InGaAsN Quantum Dots

Having created and observed InGaAsN quantum dots, we next sought to characterize optical performance of these QDs. Samples grown to study the structural formation consisted of a single, uncapped QD layer on top of the GaAs substrate. For photoluminescence (PL) measurements, a multiple layer stack of QDs were grown (Fig. 20). Multiple QD layers are used to increase the optically active volume of material. 300 Å thick GaAs barriers vertically separated the QDs. It was anticipated that the GaAs barriers were structurally relaxed such that each subsequent QD layer grew on a GaAs surface of the same nominal smoothness and quality.

As a check, an additional uncapped QD layer was deposited on the top surface of the stack such that AFM could be used to analyze QD formation.

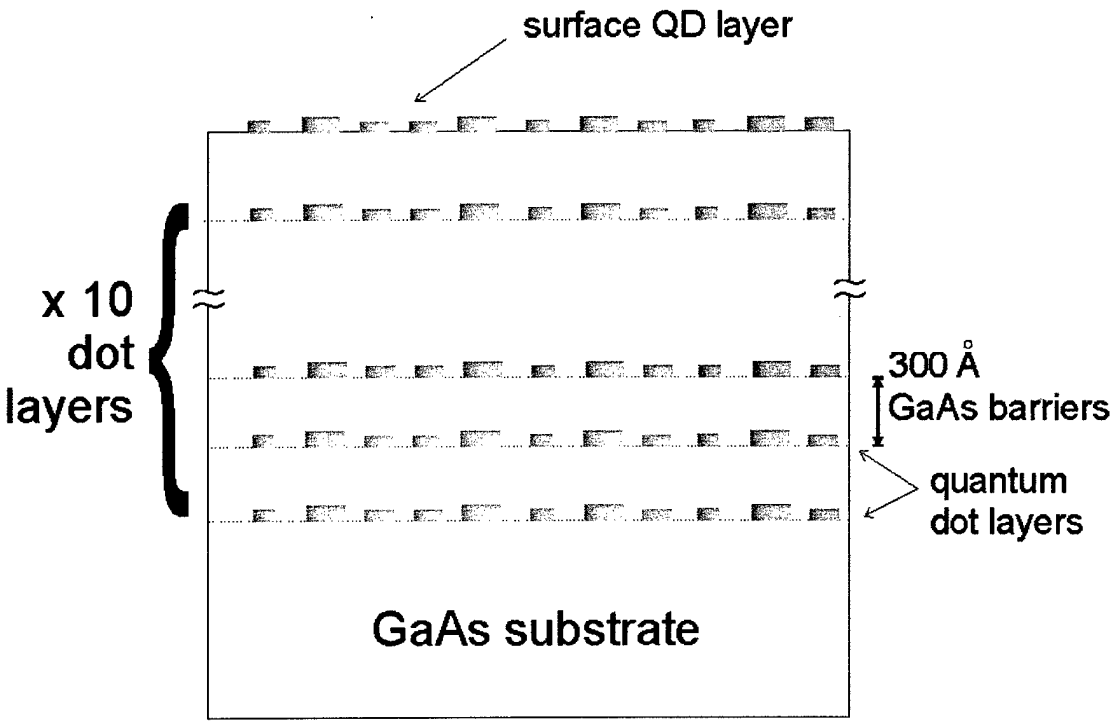

Figure 20. Schematic of multi-layer Quantum Dot stack

The first QD stack consisted of $In_{0.58}Ga_{0.42}AsN$ wetting layers, each 4 monolayers thick, with a total of 11 QD layers. GaAs 300 Å thick separated each QD layer. Substrate temperature during the stack deposition was 500 °C, and the nitrogen RF parameters were RF power = 250 W and growth pressure = 3.7 x 10^{-7} torr. As a control for comparison, the same structure was grown using $In_{0.58}Ga_{0.42}As$ only (no nitrogen).

Figure 21 displays the AFM image of the top surface of the InGaAsN QD stack. QDs are seen to be present on the surface. The RHEED pattern, which monitors surface reconstruction during growth, showed the same type of spotting for all the QD layers, including the top surface QD deposition (Fig. 22). Spotting is indicative of 3-dimensional growth on the surface, such as what occurs with QDs. Based on both the AFM and RHEED analysis, we conclude that quantum dots exist in the layers which are sandwiched between the GaAs barriers.

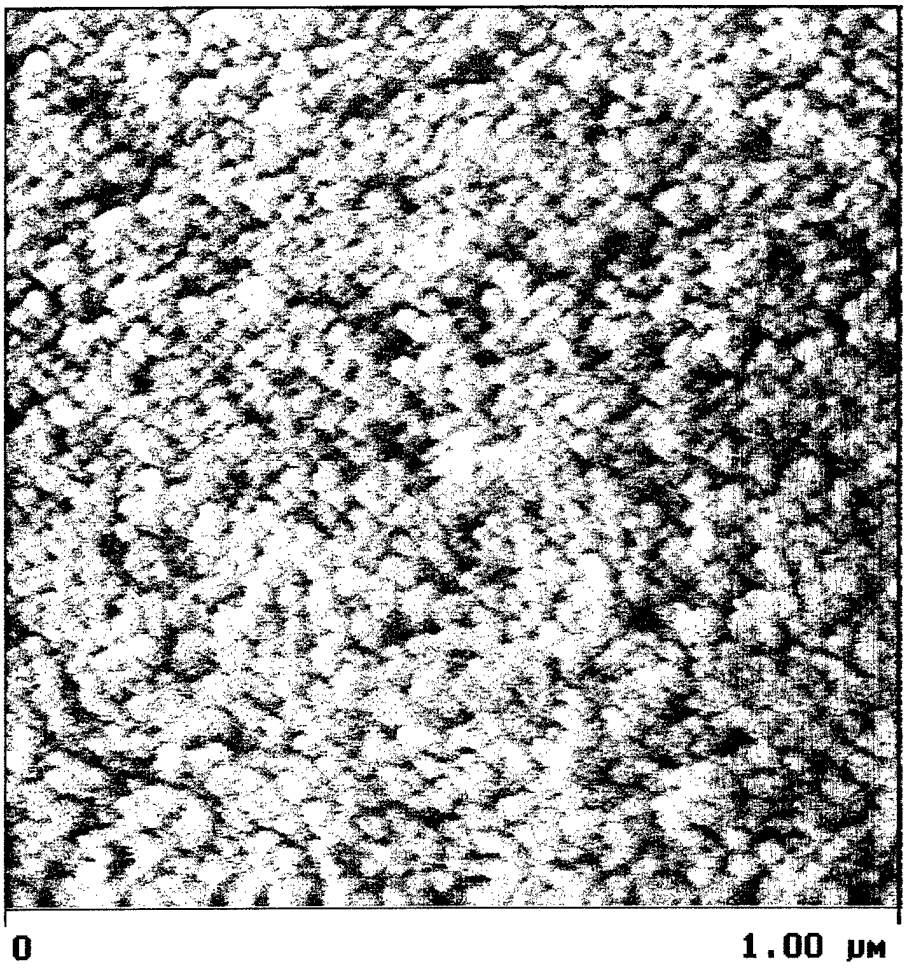

Figure 21. AFM image of 4 monolayer thick InGaAsN quantum dots on the surface of a multi-QD layer stack.

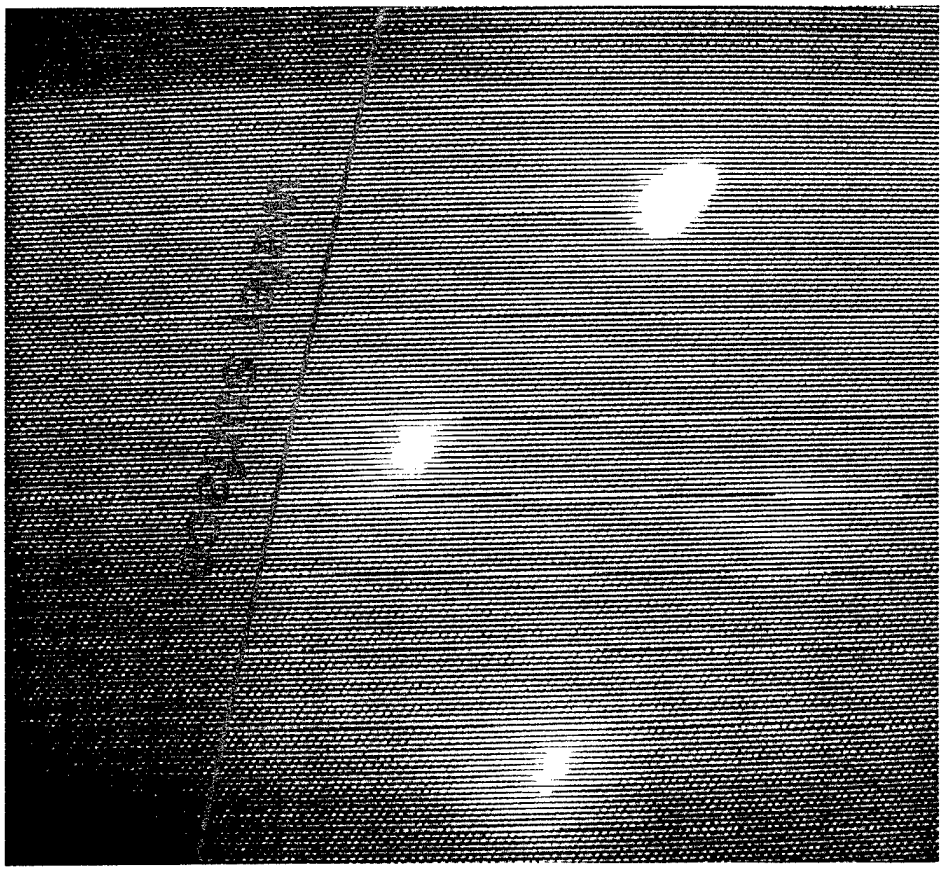

Figure 22. Photo of the RHEED image used during growth. RHEED is an in situ analytical technique used to observe the substrate surface during growth. The bright spots on the RHEED pattern indicate 3-dimensional growth, which is consistent with QD formation.

The as-grown (untreated) QD stack samples consisting of 4 monolayers InGaAs or InGaAsN were examined using photoluminescence at room temperature. Figure 23 displays the spectra for both samples. Each of the stacks has a weaker peak ~ 1260 nm. For the InGaAs-only QDs, the stronger peak is at 1010 nm, whereas the InGaAsN QDs have a peak at the slightly longer 1050 nm wavelength. Since incorporation of nitrogen is expected to lower the bandgap energy of the QD material, the 1010-1050 nm shift is evidence that nitrogen is indeed present in the InGaAsN QDs.

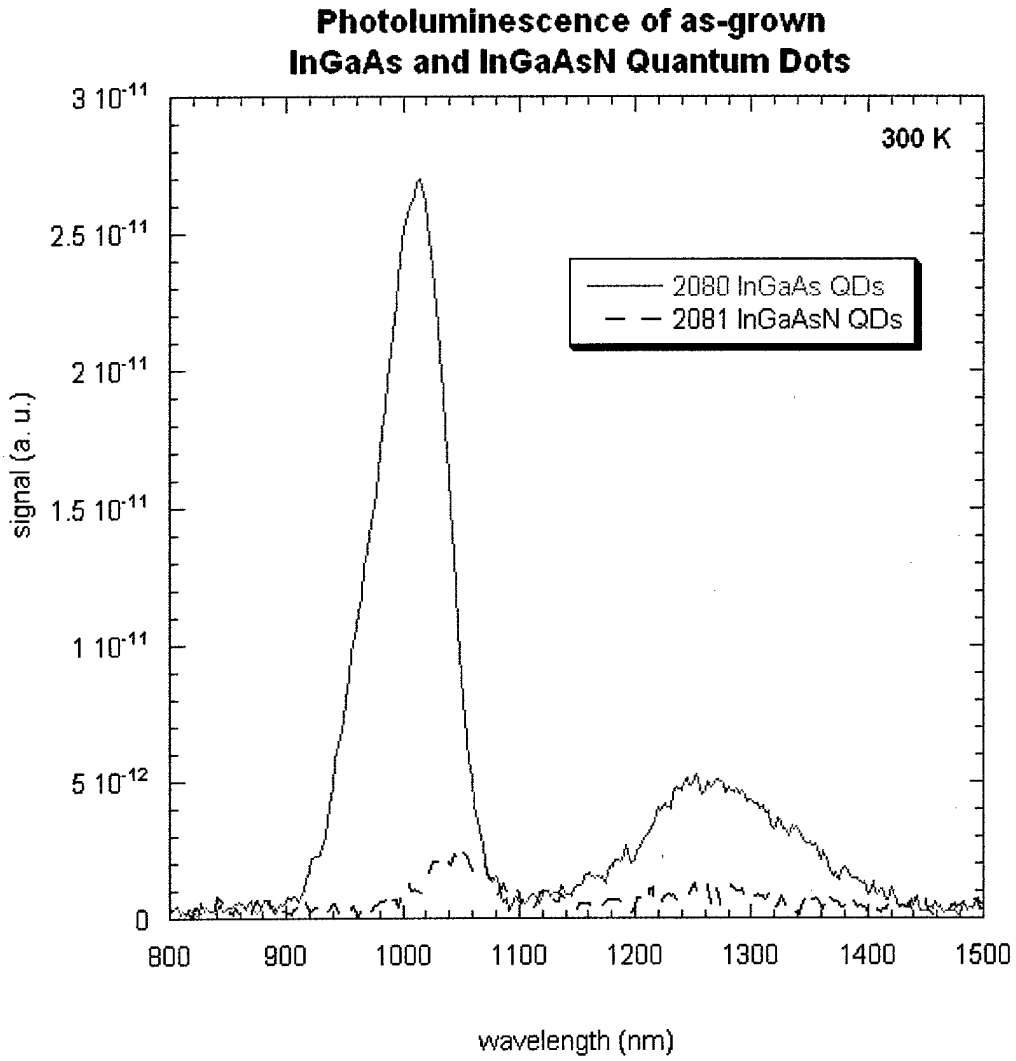

Figure 23. Room temperature photoluminescence of as-grown InGaAs and InGaAsN quantum dot stacks. Each stack consisted of 11 QD layers.

The source of the PL peaks at ~ 1260 nm isn't entirely understood. To study this further, the QD stack samples were annealed at 650 °C for 30 seconds. Annealing can reduce the defects and interface states which exist in the semiconductor crystal. Photoluminescence of the annealed samples show that the 1260 nm peak has been removed, but the 1010 and 1050 nm peaks from the InGaAs and InGaAsN QDs, respectively, are still present (Fig. 24). Thus, the 1260 nm peaks may have resulted from interface states between the QDs and the GaAs barriers, and these states were alleviated by the annealing process.

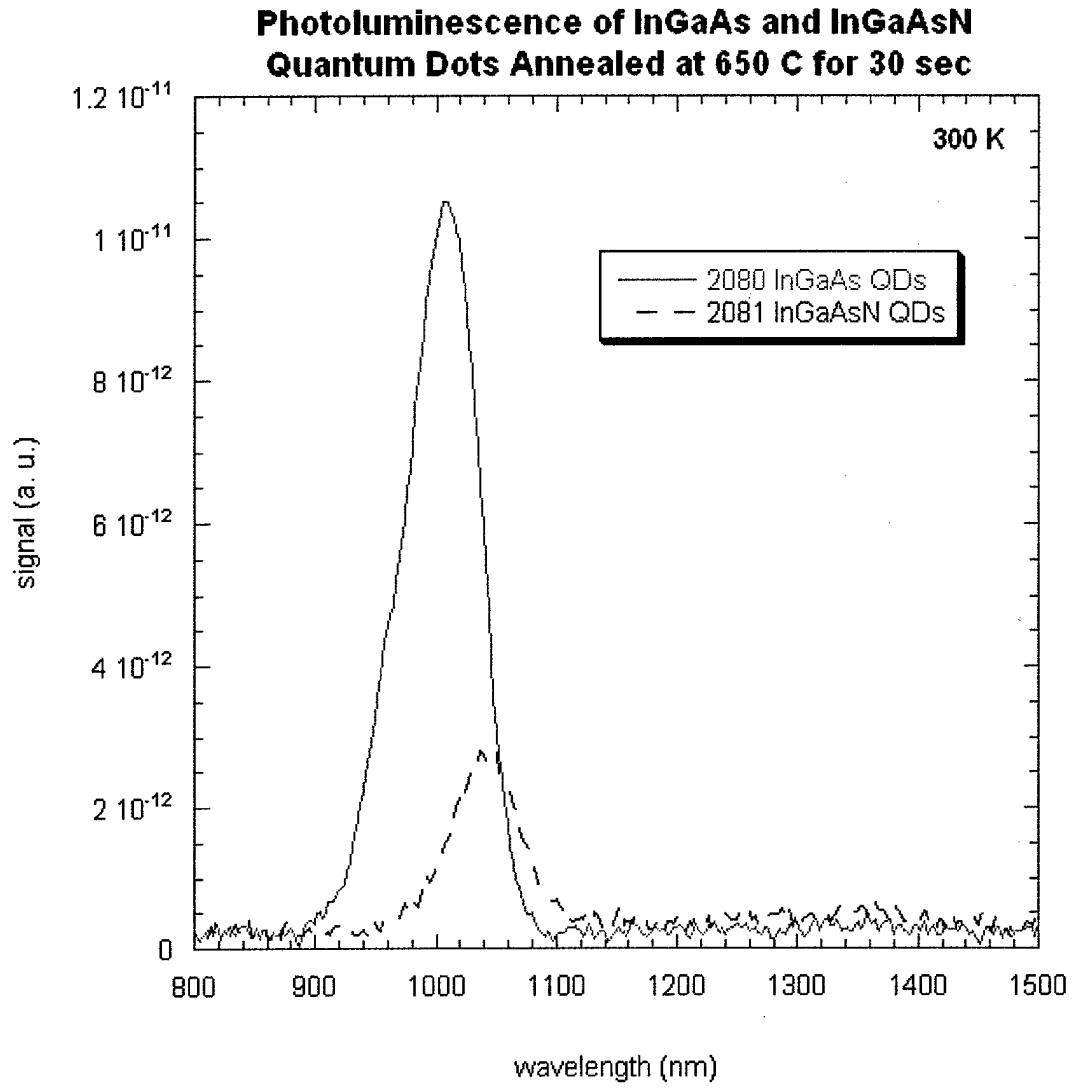

Figure 24. Room temperature photoluminescence of InGaAs and InGaAsN quantum dot stacks annealed at 650 °C for 30 seconds..

For a second series of QD stacks, the wetting layer thickness was increased to 8 monolayers. Again, InGaAsN QDs were grown on one sample, and InGaAs-only QDs were grown as a control. Substrate temperature was again 500 °C, but the nitrogen level was increased slightly (RF power 300 W and growth pressure 6.4 x 10^{-7} torr) for the InGaAsN QDs. AFM analysis of the surface of both samples showed the formation of quantum dots (Fig. 25). While most of the QDs on both samples were small (120-200 nm diameter), the InGaAsN sample did have more large diameter clusters (Fig. 6b).

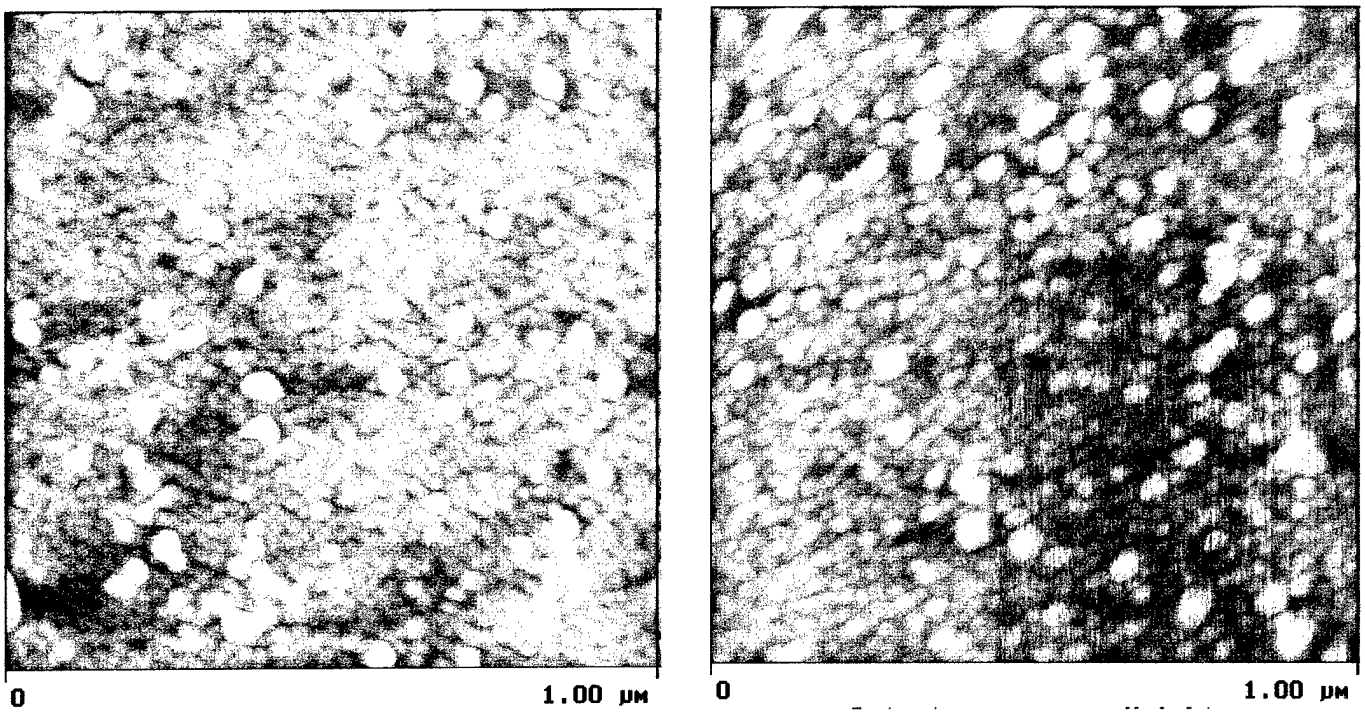

(a) (b)

Figure 25. AFM of the QD stack surface of 8 monolayer thick a) InGaAs and b) InGaAsN QDs.

The stacks were annealed prior to photoluminescence characterization. Figure 26 shows the room temperature PL spectra. The InGaAs QDs exhibit a peak ~ 1550 nm, whereas the InGaAsN QDs show a peak > 1660 nm (the detector used for the PL system starts to sharply cut off at wavelengths > 1650 nm). The peak from the InGaAsN QD also is about 50% higher than the InGaAs-only, and it had a smaller FWHM value. FWHMs were 1560 nm for the InGaAsN versus 2200 nm for the InGaAs.

PL measurements for these two stacks were also measured at 77 K (Fig. 27). The InGaAs QD peak was ~ 1480 nm, and the InGaAsN QD peak was 1540 nm. At this low temperature, the intensity of the InGaAsN QD peak was about 2.5x that of the InGaAs-only. FWHM for the InGaAs-only QDs remained ~ 2200 nm, whereas the InGaAsN QD FHWM increased to ~ 1900 nm. In both cases of room temperature and 77 K PL, the InGaAsN peaks were at a longer wavelength than the InGaAs-only control sample. Longer wavelength emission is consistent with nitrogen incorporation.

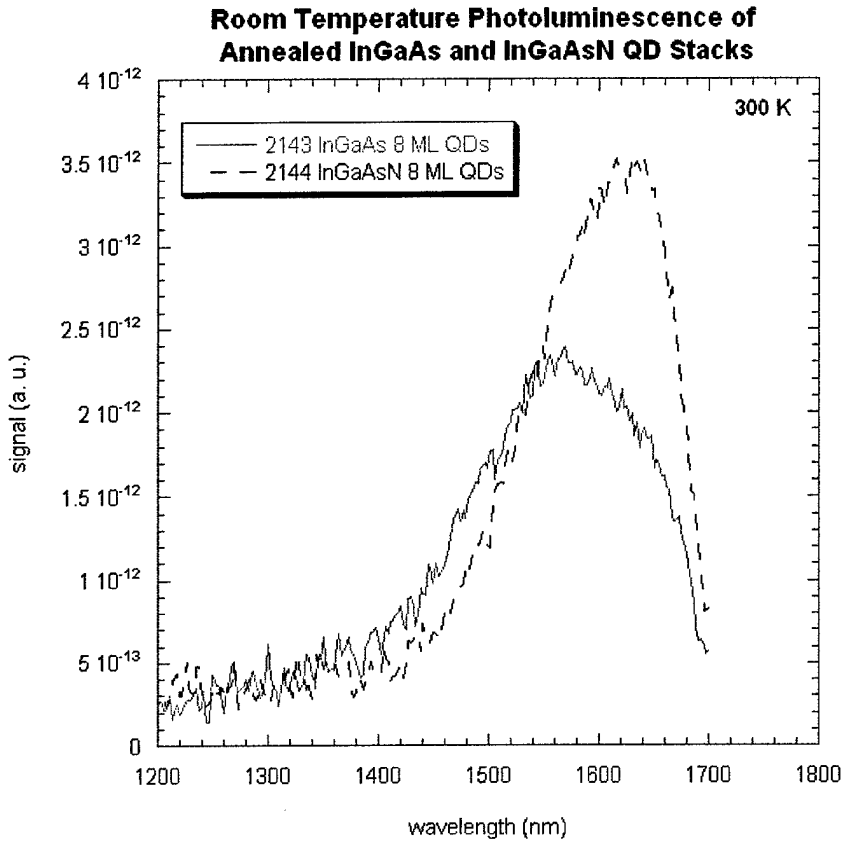

Figure 26.

Room temperature photoluminescence from InGaAs and InGaAsN QD stacks. Each QD layer consisted of 8 monolayers of deposition. Samples were annealed at 650 °C for 30 seconds.

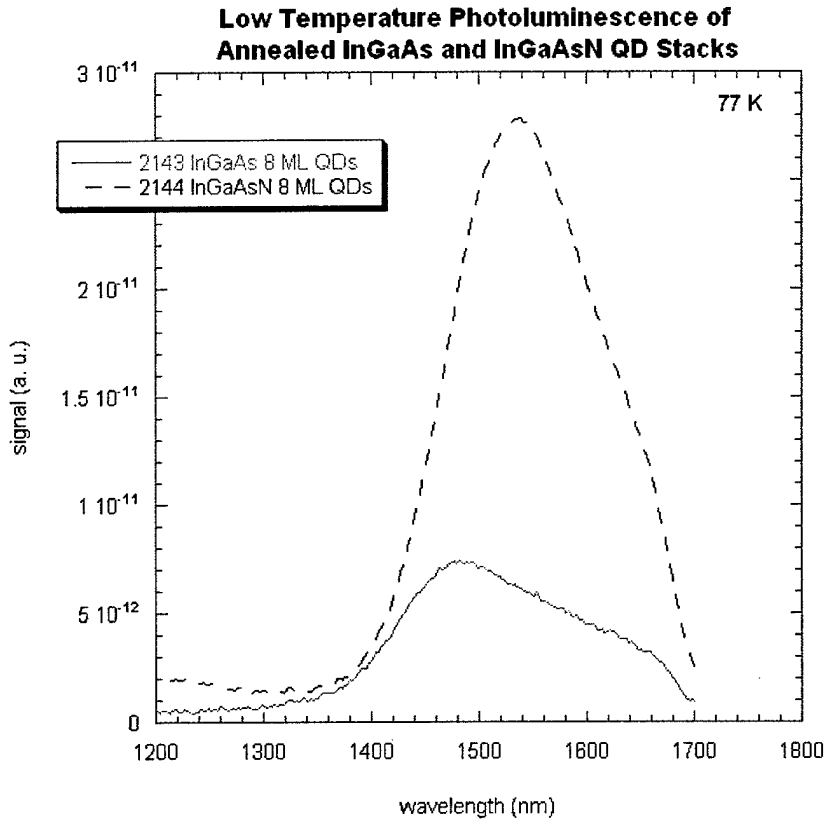

Figure 27.

Low temperature (77 K) photoluminescence from InGaAs and InGaAsN QD stacks. Each QD layer consisted of 8 monolayers of deposition. Samples were annealed at 650 °C for 30 seconds.

As a further study of these multiple layer quantum dots, these two samples were examined using high resolution transmission electron microscopy (TEM). In the large area view of sample 2143 (Fig. 28), the GaAs barriers are seen as the light grey colored areas, and the thin dark regions are the QD layers. High resolution TEM reveals dots aligning vertically (Fig. 29). Wide area TEM of the InGaAsN QD stack also displays the multiple QD layers and barriers (Fig. 30), but the close up view of the dots were inconclusive. This could be because the TEM preparation technique for InGaAsN material has not been optimized yet.

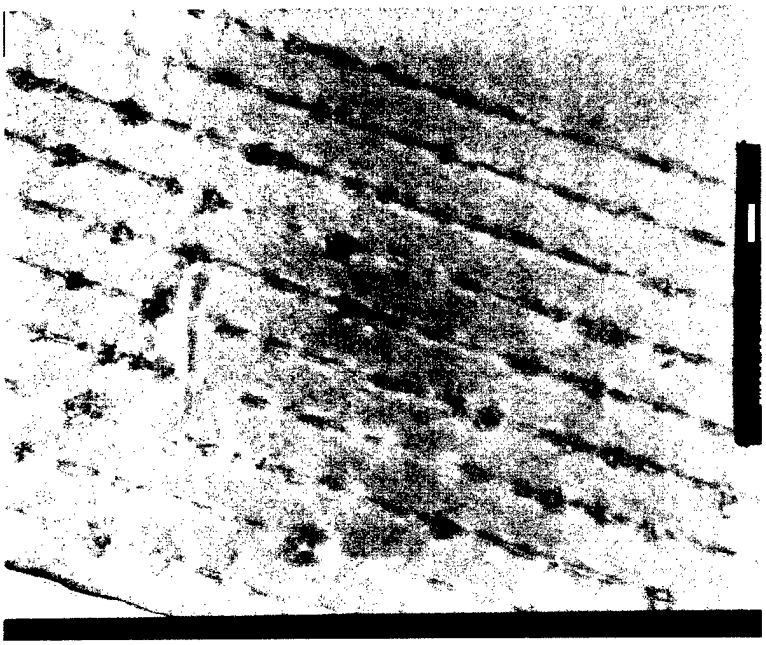

Figure 28.

High resolution TEM of InGaAs multiple layer quantum dot stack. Light grey areas are GaAs, and thin dark areas are the QD layers.

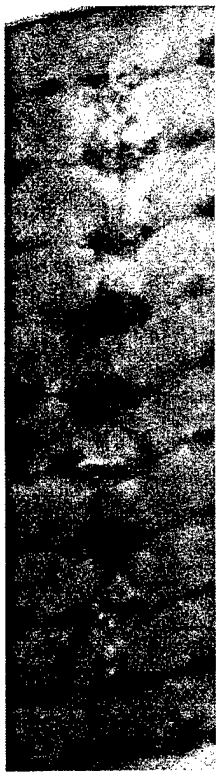

Figure 29.

Close up view of InGaAs QD stack, revealing a vertical alignment of quantum dots.

Figure 30.

High resolution TEM of InGaAsN multiple layer quantum dot stack. Light grey areas are GaAs, and thin dark areas are the InGaAsN QD layers.

Conclusion

In this Phase I study we have created and characterized InGaAsN quantum dots on GaAs substrates. We have shown that the type of substrate, on-axis versus off-axis, can influence the formation, shape and alignments of the dots. Most importantly, photonic emission from these InGaAsN QDs has been shown in the technology important 1.55 micron regime, both at 77 K and room temperature. The results of this Phase I study were highly positive and further study is warranted in a Phase II continuation. Namely, effort should continue to create infrared LEDs and laser diodes using these InGaAsN quantum dots.